# Tuning the Energy Level Offset between Donor and Acceptor with Ferroelectric Dipole Layers for Increased Efficiency in Bilayer Organic Photovoltaic Cells

*Bin Yang, Yongbo Yuan, Pankaj Sharma, Shashi Poddar, Rafal Korlacki, Stephen Ducharme, Alexei Gruverman, Ravi Saraf, and Jinsong Huang**

Organic photovoltaic (OPV) technology is one of the most attractive candidates for solving future energy problems due to its advantages of light weight, flexibility, low cost of materials and large scale production. The highest power conversion efficiency (*PCE*) of OPV devices has been increased to 8–9%.[1–7] Despite significant progress, further increasing the *PCE* to over 15% is needed for OPV to compete with silicon solar cells and other thin-film photovoltaic technologies for commercialization. The thermodynamic efficiency limit of OPV devices is 22–27%,[8,9] so there is much space for improvement. One grand challenge facing OPV device efficiency improvement is the significant energy loss incurred during the charge transfer from the donor to the acceptor, because of the energy level mismatch and the inefficient separation as well as the inefficient extraction of the bound electron-hole pairs, causing a large photovoltage loss in most OPV devices.[9,10] For example, the open circuit voltage ($V_{oc}$) in all of the reported high-efficiency (above 6%) polymeric OPV devices is less than half of the optical bandgap of the used semiconducting polymers.[1–7] The commonly accepted reason for this energy loss is that in order to obtain a required photoinduced charge transfer, the lowest unoccupied molecular orbital (LUMO) offset between the donor and the acceptor must be larger than the exciton binding energy in the donor polymer. However, it is still in doubt that there is a fundamental correlation between the polymer exciton binding energy and the energy offset needed to ensure efficient charge transfer at the donor/acceptor interface.[11] Recently the LUMO offset as small as 0.12 eV, which was even smaller than the Frenkel exciton binding energy, has been demonstrated for efficient charge transfer.[12] Therefore, there still is a huge opportunity to further increase the *PCE* of OPV devices by reducing the LUMO offset between the donor and the acceptor. For this purpose, there have been tremendous efforts to tune the energy levels of donors[1,2,4–6] and acceptors[13–16] by designing new molecule structures.

In this manuscript, we report another general method to increase the $V_{oc}$ by tuning the LUMO offset between the donor and the acceptor without changing their chemical structures. A tunable dipole layer, consisting of an ultrathin ferroelectric polymer film, was inserted between the donor and the acceptor semiconductor layers, which shifts the relative energy levels of the donor and the acceptor. The device structure and working principle of this method are shown in **Figure 1**. A polyvinylidene fluoride (70%)-trifluoroethylene (30%) copolymer, P(VDF-TrFE), was used as the tunable dipole layer. This polymer shows high polarization charge density of 100 mC $m^{-2}$ originated from the large electron affinity difference between the fluorine (F) and hydrogen (H) atoms, as shown in Figure 1a. In addition, P(VDF-TrFE) was chosen for this application due to its chemical inertness, low fabrication temperatures, photostability, and compatibility with polymer semiconducting materials. The P(VDF-TrFE) maintains its ferroelectric polarization even in films as thin as approximately 1 nm without a "finite thickness" limit.[17] In our previous study, we have demonstrated a remarkable three-fold enhancement in the *PCE* of a conventional OPV device by inserting a ferroelectric polymer layer between the active layer and the cathode to induce a strong electric field into the photoactive layer.[18] Here we show how a ferroelectric polymer layer inserted between the donor and the acceptor layers acts as tunable dipole layer to shift the energy level of semiconducting polymers.

As shown in Figure 1c-d, the relative energy levels can be tuned by a dipole layer so that the LUMO offset between the donor and the acceptor can be reduced to an optimum value for charge transfer, and then the energy difference between the highest occupied molecular orbital (HOMO) of the donor and the LUMO of the acceptor ($E_{DA}$), will be maximized. Previous studies have generally suggested that the $V_{oc}$ of OPV devices is linearly correlated with $E_{DA}$.[19,20] Therefore, the $V_{oc}$ will be increased with reduction in the LUMO offset between the donor and the acceptor. Poly(3-hexylthiophene) (P3HT) and [6,6]-phenyl-C61-butyric acid methylester (PCBM) were used for this study because they are promising candidates for the commercialized OPVs due to their excellent stability and processability by large scale deposition techniques such as gravure

B. Yang, Dr. Y. Yuan, Prof. J. Huang
Department of Mechanical and Materials Engineering and Nebraska Center for Materials and Nanoscience
University of Nebraska–Lincoln
Lincoln, Nebraska 68588-0656, USA
E-mail: jhuang2@unl.edu

P. Sharma, S. Poddar, Prof. S. Ducharme, Prof. A. Gruverman
Department of Physics and Astronomy and Nebraska Center for Materials and Nanoscience
University of Nebraska–Lincoln
Lincoln, Nebraska 68588-0299, USA

Dr. R. Korlacki, Prof. R. Saraf
Department of Chemical and Biomolecular Engineering and Nebraska Center for Materials and Nanoscience
University of Nebraska–Lincoln
Lincoln, Nebraska 68588-0643, USA

**DOI: 10.1002/adma.201104509**

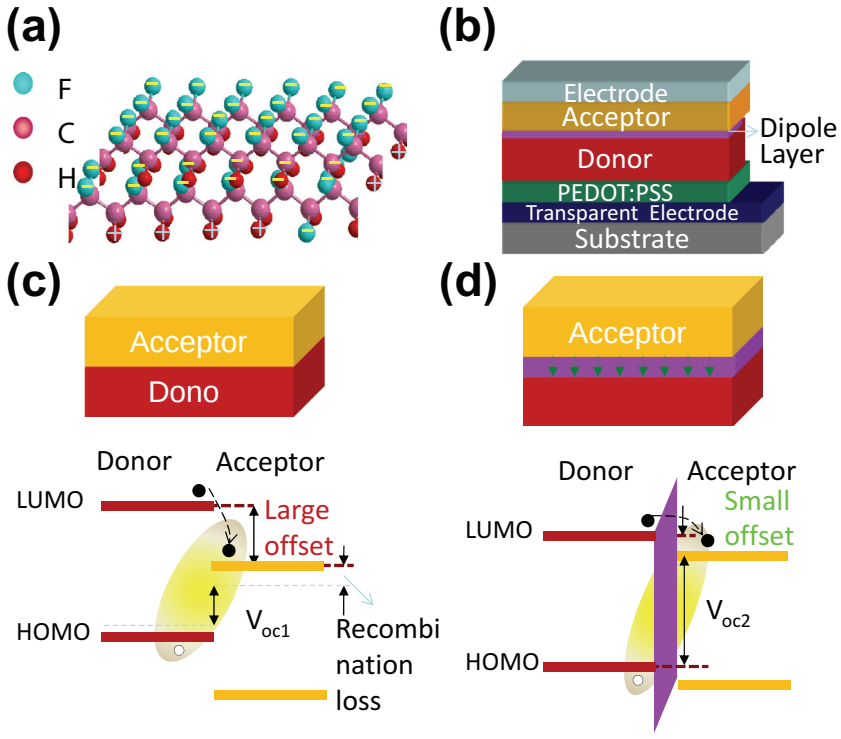


**Figure 1.** (a) The molecular structure of a ferroelectric P(VDF-TrFE) dipole layer, (b) the device structure with a dipole layer inserted between the acceptor and the donor layers, (c) and (d): the energy level diagram of the semiconductor heterostructure without and with a dipole layer inserted between the acceptor and the donor layers.

printing, spray printing etc. The P3HT/PCBM system, however, has a $V_{oc}$ output of only about 0.6 V, which is significantly lower than the optical bandgap (~2.0 eV) of P3HT. This discrepancy is caused by a very large LUMO offset close to 1.0 eV. The addition of a dipole layer presented here is a general method to improve the OPV efficiency, without the need to change the chemical structure of the active layer molecules. Therefore it is an important strategy to improve the device efficiency while preserving the advantages of the P3HT/PCBM system. In this study, the P(VDF-TrFE) layer was inserted between P3HT and PCBM bilayers by Langmuir-Blodgett (LB) deposition technique which can precisely grow the ferroelectric layer thickness by monolayer (ML) and generates P(VDF-TrFE) with excellent crystallinity, resulting in the $V_{oc}$ increase from 0.55 V to 0.67 V and two-fold increase in *PCE*, as compared to devices without aligning the dipole layer.

Efficient photoinduced charge transfer is a prerequisite for achieving efficient OPV devices. One concern that might arise is whether the increased spacing between the donor and acceptor molecules due to the inserted dipole layer would reduce the photoinduced charge transfer efficiency. It is clear that a high polarization charge density is important to afford the smallest reasonable dipole layer thickness, so that the photoinduced charge transfer through the dipole layer is efficient. The minimum required dipole layer thickness ($d$) can be estimated from polarization charge density ($\sigma_P$), dielectric constant of P(VDF-TrFE) ($\varepsilon_{FE}$), and desired energy level shift ($E$),[18]

$$d = \frac{\varepsilon_0 \varepsilon_{FE} E}{\sigma_P q} \quad (1)$$

where $\varepsilon_0$ is the vacuum dielectric constant and $q$ is the elemental electron charge. According to Equation 1, a calculated thickness as thin as 0.6 nm P(VDF-TrFE), about one monomolecular layer, is needed to induce an energy level shift of 0.8 eV (0.2 eV LUMO offset for efficient charge transfer). We expect that such a thin dipole layer will have minimal effect on the charge transfer process by tunneling. To test this hypothesis, we studied the influence of the inserted dipole layer on the efficiency of photoinduced charge transfer through photoluminescence (PL) measurements. As shown in **Figure 2**, direct contact of the P3HT layer with the PCBM layer led to a dramatically reduced PL intensity from P3HT due to the efficient photoinduced charge transfer. The decrease of PL intensity for bilayer sample P3HT/PCBM can be understood by the formation of interpenetrating donor/acceptor network by interdiffusion of PCBM into the amorphous region of P3HT matrix. In this case, the size of PCBM and the P3HT domains after interdiffusion is then within the exciton diffusion length of each material.[21,22] After inserting 1 ML P(VDF-TrFE) LB film between the P3HT layer and the PCBM layer, the PL intensity was found to reduce further. This result demonstrates that the inserting 1 ML P(VDF-TrFE) LB film does not hinder photoinduced charge transfer from the donor to the acceptor due to its small average thickness of 1.7 nm; instead, it appears to improve the photoinduced charge transfer. One possible reason is that the LUMO offset is larger than the molecule reorganization

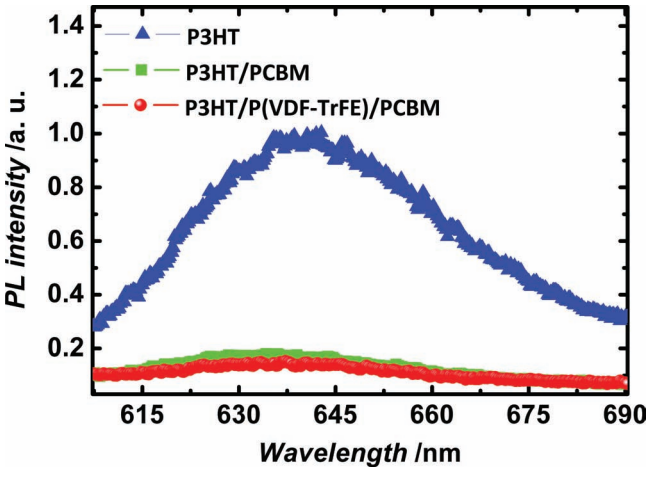


**Figure 2.** PL intensity from a plain P3HT layer (blue triangles), a bilayer film with structure of PCBM on P3HT layer (green squares), and a trilayer film with structure of 1 ML P(VDF-TrFE) inserted between P3HT and PCBM layers (red balls). The light was incident from the PCBM side.

energy, entering the so-called "inverted" region of Marcus theory, resulting in an increased electron transfer rate.[23]

The device performance was significantly improved after addition of the ferroelectric dipole layer of P(VDF-TrFE), as shown in **Figure 3**a. The short circuit current density ($J_{sc}$), $V_{oc}$, fill factor (*FF*), and *PCE* of the resulting trilayer device were 8.2 mA cm$^{-2}$, 0.55 V, 33% and 1.5%, respectively, which are typical values for bilayer P3HT/PCBM OPV devices.[21,24] The $V_{oc}$ was increased from 0.55 V to 0.67 V after poling the P(VDF-TrFE) layer by applying a reverse bias on the device. The dipoles can preserve their alignment after removing the bias, which is the unique property of a ferroelectric film.[17,25] This $V_{oc}$ of 0.67 V is significantly larger than values reported either in bilayer or bulk heterojunction OPV devices based on P3HT/PCBM as active layers.[21,24,26] An increase in $J_{sc}$ of 0.8 mA cm$^{-2}$ was also observed after poling the P(VDF-TrFE) LB film by a reverse bias. The *FF* was enhanced from 33% to 55%. Thus, the *PCE* was more than doubled from 1.5% to 3.3%. It is expected the efficiency will be further increased by replacing PCBM with [6,6]-phenyl-C71 butyric acid methyl ester ($PC_{70}BM$) or indene-$C_{60}$ bisadduct (ICBA).[16]

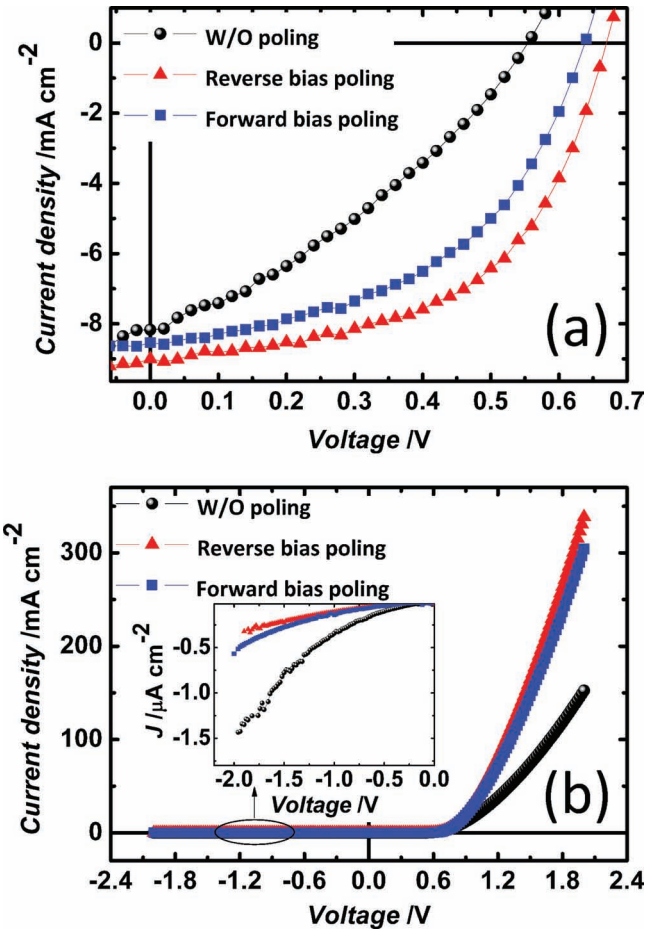


**Figure 3.** Device performance variation with the insertion of 1 ML P(VDF-TrFE) dipole layer between P3HT and PCBM layers: (a) *J–V* curves under the simulated Air Mass 1.5 Global Irradiation (100 mW cm$^{-2}$) for the as made trilayer device (black balls), after poling the P(VDF-TrFE) layer with reverse bias (red triangles) and forward bias pulses (blue squares), respectively; (b) *J–V* curves in dark of the device under the three poling conditions.

A unique feature of using a ferroelectric film as the dipole layer is that its polarization direction is bistable and it can be switched between opposite states by a voltage pulse. This tunability is clearly demonstrated by the data as shown in Figure 3a. The black circles show the photovoltaic characteristics before poling the P(VDF-TrFE) film. After poling the ferroelectric P(VDF-TrFE) film by a large reverse bias of –16 V, all of the photovoltaic device characteristics $V_{oc}$, *FF* and $J_{sc}$ were greatly improved. In contrast, after poling the ferroelectric P(VDF-TrFE) film by forward bias +2 V, the photovoltaic characteristics were reduced as compared to the reverse bias poled state. Here a relative small forward bias of +2 V was applied for poling to avoid the burning of the devices by the high current density at forward bias. There is no such problem for the reverse bias poling because our devices are diodes. Therefore it is very likely that the ferroelectric dipole was only partially switched by the +2 V poling, which explains the small difference in current-voltage (*J–V*) curves between the reverse bias and forward bias poling. The photocurrent can be switched between these two states repeatedly. This reproducible switching behavior is most likely caused by the ferroelectric phase of P(VDF-TrFE) film rather than the claimed electrochemical reaction,[27] which will be demonstrated in the following part of this manuscript.

In addition to the tunable photocurrent, the dark current of the devices was also tuned by polarization of the dipole layer, as shown in Figure 3b. The dark current reduced by a factor of four after reverse bias poling the ferroelectric dipole layer. This reduction in dark current is also due to the tuning of energy levels by poling the ferroelectric dipole layer with reverse bias. Previous study found that the dark current in bilayer OPV devices originates from the thermal activation of the electrons from the HOMO of the donor to the LUMO of the acceptor with an activation energy of $E_{DA}$. This can be understood from the general expression for $V_{oc}$ in OPV devices:[28–32]

$$V_{oc} = \frac{nkT}{q}\ln\left(\frac{J_{sc}}{J_0}+1\right) \approx \frac{nkT}{q}\ln\left(\frac{J_{sc}}{J_0}\right) \quad (2)$$

$$J_0 = J_{00}\exp\left(\frac{-E_{DA}}{nkT}\right) \quad (3)$$

where $k$ is the Boltzmann constant, $T$ is temperature, $q$ is the elemental electron charge, $J_0$ is the saturated dark current density, $J_{00}$ is a factor for recombination of charge transfer excitons (CTEs) which are the bound electron-hole pairs, and $n$ is the diode ideality factor. As shown in Figure 1c,d, the value of $E_{DA}$ increases with the insertion of the dipole layer between the donor and the acceptor layers by shifting the LUMO of acceptor upwards. According to Equations 2 and 3, the inserted dipole layer can reduce the saturated dark current density and thus increase the correlated $V_{oc}$ by increasing $E_{DA}$ after reverse bias poling the dipole layer. Additionally, the inserted dipole layer can also reduce the electronic coupling between the donor and the acceptor molecules by increasing the spacing between them, and hence reduce the recombination of CTEs. The reduced recombination of CTEs is reflected by a reduction in $J_{00}$, which therefore results in additional $V_{oc}$ enhancement. It is not straightforward to explain the increases in $J_{sc}$ and *FF* observed after poling the

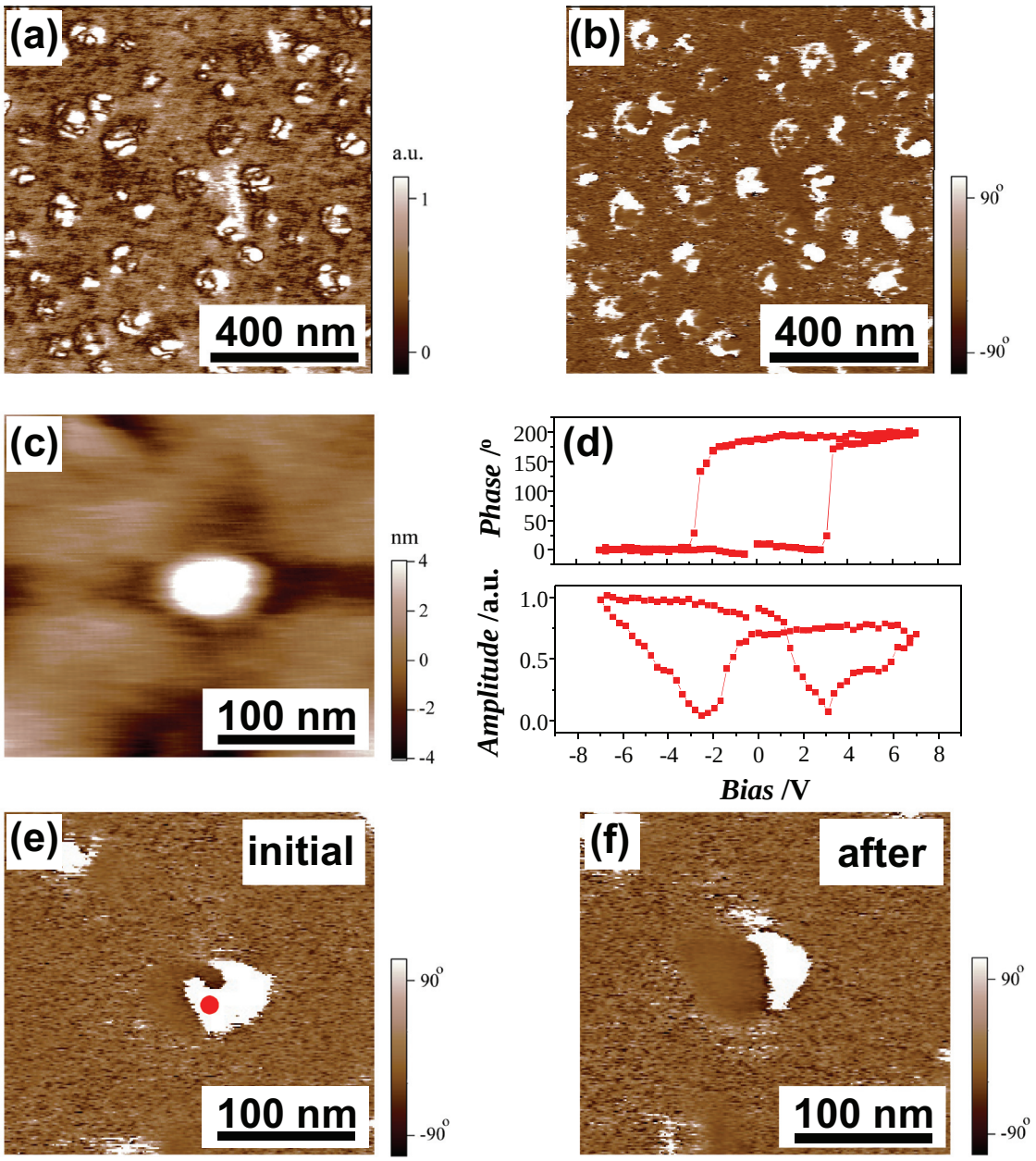


**Figure 4.** (a, b) PFM images of ferroelectric P(VDF-TrFE) nanoislands sandwiched between P3HT layer and PCBM layer (1.0 μm × 1.0 μm): (a) PFM amplitude, (b) PFM phase. (c-f) show the ferroelectric switching of a P(VDF-TrFE) nanoisland: (c) topographic image of a single P(VDF-TrFE) nanoisland; (d) PFM hysteresis loops (phase and amplitude) of the P(VDF-TrFE) nanoisland; (e, f) PFM phase images of the P(VDF-TrFE) nanoisland before and after applying the voltage pulse (–6 V, 2 s). The red dot in (e) marks the location of the PFM tip during voltage pulse application.

dipole layer within the theoretical frame of the energy levels, but it can be well understood by the reduced CTEs recombination which generally results in increases in $J_{sc}$ and *FF*.

Although the $V_{oc}$ of 0.67 V is significantly higher than what achieved in optimized bilayer or bulk heterojunction P3HT/PCBM OPV devices, it is still far less than the maximum attainable $V_{oc}$ of 1.5 V which assumes LUMO offset 0.2 V loss for the efficient charge transfer and a $V_{oc}$ loss of 0.3 V due to the non-ideal diode[20] in P3HT/PCBM OPV devices. In order to find out the reason for such huge discrepancy, piezoresponse force microscopy (PFM) measurements were conducted on the tri-layer samples with the insertion of 1 ML P(VDF-TrFE) between the PCBM film and the P3HT film, to reveal the morphology and ferroelectric state of this dipole layer. PFM has the unique capability to measure the local piezoelectric response, not only on the surface but also for layers embedded under the thin PCBM layer (~20 nm) or under a thin layer of metal.[33] The piezoelectric response is related to the net electric polarization and is therefore a good local probe of the polarization state.[34,35] It was clearly evident from **Figure 4**a,b that only approximately

20% of the P3HT surface was covered by the ferroelectric P(VDF-TrFE) nanoislands because P(VDF-TrFE) tends to shrink on P3HT surface after thermal annealing. This is due to the large surface energy mismatch between these two materials: 51 mJ $m^{-2}$ for P(VDF-TrFE)[36] and 26.9 mJ $m^{-2}$ for P3HT.[37] A three-dimensional growth mode is preferred for P(VDF-TrFE) on P3HT to minimize the surface energy. This local piezoelectric response of the P(VDF-TrFE) grains embedded under thin PCBM layer confirmed that the inserted P(VDF-TrFE) layer was in the ferroelectric state which is crucial for maintaining a permanent polarization. The ferroelectricity of the P(VDF-TrFE) nanoislands was further confirmed by the direct observation of their polarization by applying pulse voltage between the PFM tip and the P(VDF-TrFE) nanoislands. The typical PFM phase and amplitude hysteresis loops obtained for the P(VDF-TrFE) grain on P3HT were shown in Figure 4c,d. It was found that the reverse coercive bias is –2.6 V while the forward coercive bias is +3 V. As clearly shown in Figure 4e,f, the polarization direction of P(VDF-TrFE) dipoles was reversed after applying a reverse bias of –6 V.

The low coverage (~20%) of P(VDF-TrFE) on P3HT layer should lead to the direct contact of P3HT and PCBM, and explains the much lower $V_{oc}$ than the theoretical limit. The observed $V_{oc}$ is the average $V_{oc}$ of all the nanometer-sized OPV devices connected in parallel. Further improvement of the device performance by this method then requires a better control of the P(VDF-TrFE) film morphology for a higher coverage and uniform thickness on P3HT which is in our current study. It is speculated that if the coverage of 100% ferroelectric P(VDF-TrFE) on P3HT layer can be obtained, the $V_{oc}$ is expected to be tuned up to about 1.0-1.5 V in the P3HT/PCBM OPV devices.

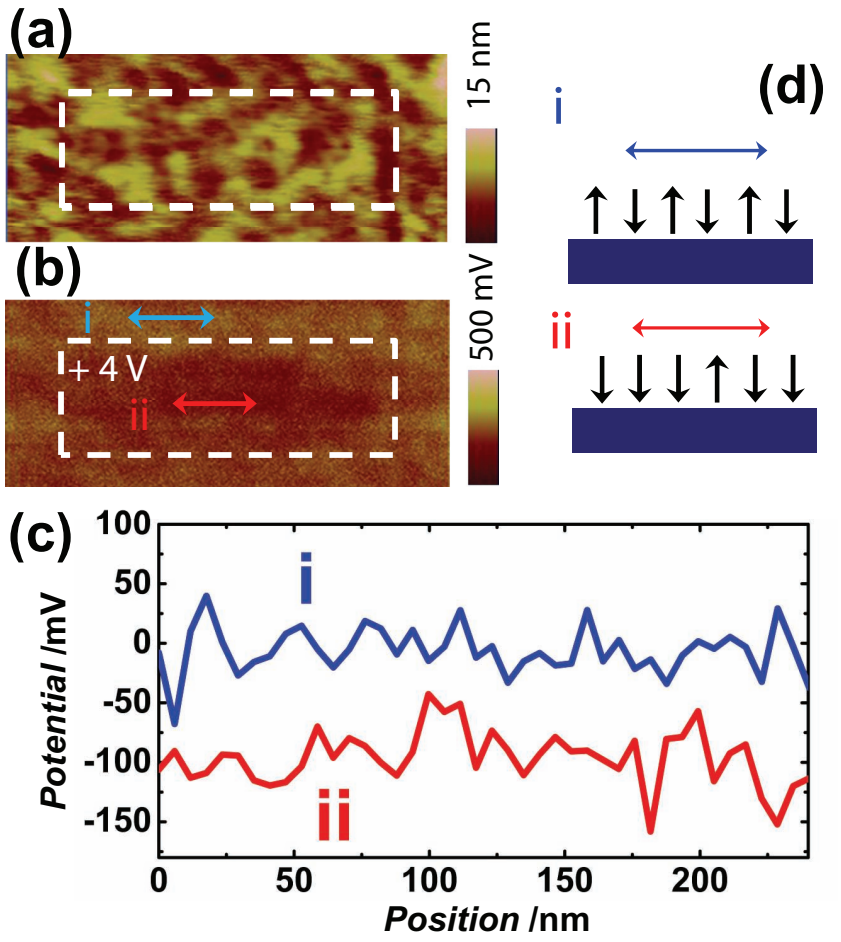


**Figure 5.** (a) topography and (b) surface potential map of the P(VDF-TrFE) film, where the area was marked by a white rectangle was poled by a +4 V direct-current voltage applied by the PFM tip (Image size is 1.0 μm × 3.0 μm), (c) cross-sectional analysis of the surface potential map along the **i** and **ii** lines as labeled in (b), (d) schematic illustration of the origin of the potential difference.

The tuning of the relative energy levels of the P3HT and the PCBM was confirmed by the electrostatic force microscopy (EFM) (**Figure 5**). In this measurement, a forward bias of +4 V was applied between the EFM tip and the film substrate to align the dipoles in a rectangle area in a contact mode, and the potential image of the whole film was measured in a non-contact mode with a small bias of 0.2 V on the EFM tip. The topography was not found to change after the poling process. It was clearly observed that the electrical potential on the P(VDF-TrFE) surface polarized by +4 V bias was tuned to be 100 mV lower by the applied bias (the deeper color in Figure 5b). The charging of the insulating P(VDF-TrFE) polymer by the EFM tip can be ruled out because it will generate a higher potential in the poled region (i.e. positive charges will be left on the P(VDF-TrFE) surface). This potential difference is then concluded to be resulted from the reversal of the electrical dipoles in P(VDF-TrFE) film, as illustrated in the Figure 5d. The average surface potential difference is 0.1 V, which is consistent with tuned $V_{oc}$. The fluctuation of surface potential is consistent with the nonuniform distribution of the ferroelectric P(VDF-TrFE) nanoislands on P3HT layer. The peak to valley potential difference reaches 0.3 V, or maybe even higher which is not shown due to the low resolution of the EFM scanning (50 nm in our case). Again this result indicates a large potential to further increase the energy tuning capability by the ferroelectric dipoles with increased coverage of the dipole layer.

In conclusion, we demonstrated a method to increase the $V_{oc}$ of bilayer OPV devices by tuning the energy level offset of the donor and the acceptor with tunable ferroelectric P(VDF-TrFE) dipole layers. Additionally, both $J_{sc}$ and *FF* also increased due to the reduced recombination loss of CTEs. Thus, a double efficiency was achieved for P3HT and PCBM based bilayer OPV devices. We expect that a further increase of $V_{oc}$ can be achieved by improving the coverage of the P(VDF-TrFE) dipole layer on P3HT. The $V_{oc}$ can be potentially improved to above 1.0 V

without compromising other photovoltaic parameters such as $J_{sc}$ and *FF*.

## Experimental Section

A cleaned indium tin oxide (ITO)/glass substrate was firstly treated by ultraviolet-ozone for 10 min. Poly(3,4-ethylenedioxythiophene):poly(styrenesulfonate) (PEDOT:PSS) (Baytron-P 4083) was then spin-coated onto it at a spin speed of 3500 rpm, which produced a PEDOT:PSS film thickness of approximately 30 nm, as measured with a Dektak profilometer. After that, the PEDOT:PSS film was baked at 125 °C for 30 min. Subsequently, the P3HT (Rieke, used as received) which was pre-dissolved in 1,2-dichlorobenzene to form a solution (concentration of 20 mg $mL^{-1}$), was spin-coated onto PEDOT:PSS film at a spin speed of 1000 rpm for 25 s followed by 2000 rpm for 35 s to form a layer thickness of around 80 nm.[21] Then, an ultrathin P(VDF-TrFE 70:30) dipole layer was coated onto the P3HT layer by LB deposition and then annealed at 135 °C for 30 min, the detailed fabrication process was stated elsewhere.[18] Subsequently, the PCBM (Nano-C, used as received, 5 mg $mL^{-1}$) pre-dissolved in dichloromethane was then spin-coated onto the obtained film and then annealed at 140 °C for 20 min. The device fabrication was finalized by thermally evaporating calcium of thickness 10 nm as cathode and then covered by 100 nm thick aluminum. The active device area was approximately 0.07 $cm^2$. Photocurrent was measured under simulated air mass 1.5 global irradiation (100 mW $cm^{-2}$).

The PL measurements were performed using a commercial spectrophotometer (F-4500, Hitachi Inc.) equipped with the standard solid sample holder. The excitation light was provided by a Xenon lamp and restricted to a spectral window of 480 ± 2.5 nm. The photoluminescence emission from the sample was dispersed by a grating and the photoluminescence spectra recorded with a speed of 60 nm $minute^{-1}$ using a photomultiplier tube (R3788, Hamamatsu Photonics K.K.) operated at 700 V.

For the EFM measurements, the ITO layer on the bottom was grounded and the sample was scanned by a platinum (Pt) tip in tapping mode during the poling process. A positive direct-current voltage of +4 V was applied on the Pt tip when the tip entered the target region. The whole poling process took about 10 min. After the poling process, a surface potential image was obtained by scanning the sample again in the same region.

## Acknowledgements

J. Huang acknowledges partial support of this work by the Defense Threat Reduction Agency, Basic Research Award No. HDTRA1-10-1-0098 and National Science Foundation MRSEC Program, and the Nebraska Research Initiative. P. Sharma and A. Gruverman acknowledge the support of U. S. Department of Energy under Award DE-SC0004530.

Received: November 25, 2011
Revised: December 28, 2011
Published online: February 13, 2012

[1] C. M. Amb, S. Chen, K. R. Graham, J. Subbiah, C. E. Small, F. So, J. R. Reynolds, *J. Am. Chem. Soc.* **2011**, *133*, 10062.
[2] H. Y. Chen, J. Hou, S. Zhang, Y. Liang, G. Yang, Y. Yang, L. Yu, Y. Wu, G. Li, *Nat. Photonics* **2009**, *3*, 649.
[3] Z. He, C. Zhong, X. Huang, W. Y. Wong, H. Wu, L. Chen, S. Su, Y. Cao, *Adv. Mater.* **2011**, *23*, 4636.
[4] Y. Liang, Z. Xu, J. Xia, S. T. Tsai, Y. Wu, G. Li, C. Ray, L. Yu, *Adv. Mater.* **2010**, *22*, E135.
[5] S. Loser, C. J. Bruns, H. Miyauchi, R. Ponce Ortiz, A. Facchetti, S. I. Stupp, T. J. Marks, *J. Am. Chem. Soc.* **2011**, *133*, 8142.
[6] S. H. Park, A. Roy, S. Beaupr, S. Cho, N. Coates, J. S. Moon, D. Moses, M. Leclerc, K. Lee, A. J. Heeger, *Nat. Photonics* **2009**, *3*, 297.
[7] S. C. Price, A. C. Stuart, L. Yang, H. Zhou, W. You, *J. Am. Chem. Soc.* **2011**, *133*, 4625.
[8] N. C. Giebink, G. P. Wiederrecht, M. R. Wasielewski, S. R. Forrest, *Phys. Rev. B* **2011**, *83*, 195326.
[9] T. Kirchartz, K. Taretto, U. Rau, *J. Phys. Chem. C* **2009**, *113*, 17958.
[10] K. Vandewal, K. Tvingstedt, J. V. Manca, O. Inganäs, *IEEE J. Sel. Top. Quantum Electron.* **2010**, *16*, 1676.
[11] S. Cook, R. Katoh, A. Furube, *J. Phys. Chem. C* **2009**, *113*, 2547.
[12] X. Gong, M. Tong, F. G. Brunetti, J. Seo, Y. Sun, D. Moses, F. Wudl, A. J. Heeger, *Adv. Mater.* **2011**, *23*, 2272.
[13] Y. J. Cheng, C. H. Hsieh, Y. He, C. S. Hsu, Y. Li, *J. Am. Chem. Soc.* **2010**, *132*, 17381.
[14] P. P. Khlyabich, B. Burkhart, B. C. Thompson, *J. Am. Chem. Soc.* **2011**, *133*, 14534.
[15] E. Voroshazi, K. Vasseur, T. Aernouts, P. Heremans, A. Baumann, C. Deibel, X. Xue, A. J. Herring, A. J. Athans, T. A. Lada, *J. Mater. Chem.* **2011**, *21*, 17345.
[16] G. Zhao, Y. He, Y. Li, *Adv. Mater.* **2010**, *22*, 4355.
[17] A. V. Bune, V. M. Fridkin, S. Ducharme, L. M. Blinov, S. P. Palto, A. V. Sorokin, S. G. Yudin, A. Zlatkin, *Nature* **1998**, *391*, 874.
[18] Y. Yuan, T. J. Reece, P. Sharma, S. Poddar, S. Ducharme, A. Gruverman, Y. Yang, J. Huang, *Nat. Mater.* **2011**, *10*, 296.
[19] C. J. Brabec, A. Cravino, D. Meissner, N. S. Sariciftci, T. Fromherz, M. T. Rispens, L. Sanchez, J. C. Hummelen, *Adv. Funct. Mater.* **2001**, *11*, 374.
[20] M. C. Scharber, D. Mühlbacher, M. Koppe, P. Denk, C. Waldauf, A. J. Heeger, C. J. Brabec, *Adv. Mater.* **2006**, *18*, 789.
[21] K. H. Lee, P. E. Schwenn, A. R. G. Smith, H. Cavaye, P. E. Shaw, M. James, K. B. Krueger, I. R. Gentle, P. Meredith, P. L. Burn, *Adv. Mater.* **2010**, *23*, 766.
[22] N. D. Treat, M. A. Brady, G. Smith, M. F. Toney, E. J. Kramer, C. J. Hawker, M. L. Chabinyc, *Adv. Energy Mater.* **2011**, *1*, 82.
[23] R. A. Marcus, *Rev. Mod. Phys.* **1993**, *65*, 599.
[24] V. S. Gevaerts, L. J. A. Koster, M. Wienk, R. A. J. Janssen, *ACS Appl. Mater. Interfaces* **2011**, *3*, 3252.
[25] V. Fridkin, A. Ievlev, K. Verkhovskaya, G. Vizdrik, S. Yudin, S. Ducharme, *Ferroelectrics* **2005**, *314*, 37.
[26] G. Li, V. Shrotriya, J. Huang, Y. Yao, T. Moriarty, K. Emery, Y. Yang, *Nat. Mater.* **2005**, *4*, 864.
[27] K. Asadi, P. de Bruyn, P. W. M. Blom, D. M. de Leeuw, *Appl. Phys. Lett.* **2011**, *98*, 183301.
[28] W. J. Potscavage, S. Yoo, B. Kippelen, *Appl. Phys. Lett.* **2008**, *93*, 193308.
[29] K. Vandewal, K. Tvingstedt, A. Gadisa, O. Inganäs, J. V. Manca, *Nat. Mater.* **2009**, *8*, 904.
[30] P. Erwin, M. E. Thompson, *Appl. Phys. Lett.* **2011**, *98*, 223305.
[31] N. Li, B. E. Lassiter, R. R. Lunt, G. Wei, S. R. Forrest, *Appl. Phys. Lett.* **2009**, *94*, 023307.
[32] B. Yang, J. Cox, Y. Yuan, F. Guo, J. Huang, *Appl. Phys. Lett.* **2011**, *99*, 133302.
[33] A. Gruverman, *J. Mater. Sci.* **2009**, *44*, 5182.
[34] A. V. Bune, C. Zhu, S. Ducharme, L. M. Blinov, V. M. Fridkin, S. P. Palto, N. G. Petukhova, S. G. Yudin, *J. Appl. Phys.* **1999**, *85*, 7869.
[35] P. Sharma, T. J. Reece, S. Ducharme, A. Gruverman, *Nano Lett.* **2011**, *11*, 1970.
[36] S. Wi, N. Senthilkumar, S. W. Rhee, *J. Mater. Sci. Mater. Electron.* **2008**, *19*, 45.
[37] D. S. Germack, C. K. Chan, B. H. Hamadani, L. J. Richter, D. A. Fischer, D. J. Gundlach, D. M. DeLongchamp, *Appl. Phys. Lett.* **2009**, *94*, 233303.